Plant intracellular innate immune receptor Resistance to *Pseudomonas syringae pv. maculicola 1* (RPM1) is activated at, and functions on, the plasma membrane

Zhiyong Gao[a], Eui-Hwan Chung[a], Timothy K. Eitas[a,b,c], and Jeffery L. Dangl[a,b,c,d,1]

[a]Department of Biology, [b]Curriculum in Genetics and Molecular Biology, [c]Department of Microbiology and Immunology, and [d]Carolina Center for Genome Sciences, University of North Carolina, Chapel Hill, NC 27599

Contributed by Jeffery L. Dangl, March 21, 2011 (sent for review March 7, 2011)

Plants deploy intracellular innate immune receptors to recognize pathogens and initiate disease resistance. These nucleotide-binding, leucine-rich repeat (NB-LRR) proteins are activated by pathogen effector proteins that are delivered into the host cell to suppress host defense responses. Little is known about the sites and mechanisms of NB-LRR activation, but some NB-LRR proteins can function inside the plant nucleus. We demonstrate that RPM1 is activated on the plasma membrane and does not relocalize to the nucleus. An autoactive RPM1(D505V) allele that recapitulates key features of normal RPM1 activation also resides on the plasma membrane. There is no detectable relocalization of activated RPM1 to the nucleus. Hindering potential nuclear entry of RPM1-Myc did not affect either its effector-triggered hypersensitive-response (HR) cell death or its disease resistance functions, further suggesting that nuclear translocation is not required for RPM1 function. RPM1 tethered onto the plasma membrane with a dual acylated N-terminal epitope tag retained the ability to mediate HR, consistent with this RPM1 function being activated on the plasma membrane. Plant NB-LRR proteins can thus function at various locations in the cell.

plant disease resistance | plant nucleotide-binding leucine-rich repeat receptor immune receptor | type III bacterial effectors

Plants use a two-tiered receptor-based immune system to prevent the invasion of pathogenic microorganisms (1, 2). Plants express transmembrane pattern recognition receptors to detect microbe-associated molecular patterns (MAMPs). This leads to intracellular signaling and transcriptional output responses that can halt the growth of nonpathogens and is termed MAMP-triggered immunity (MTI). Successful pathogens suppress or dampen MTI via delivery of "effector proteins" into the host cell. Hence, effectors are virulence factors. To counter the activities of effector proteins, plants deploy polymorphic intracellular receptors. The largest class of these receptors, composed of nucleotide-binding, leucine-rich repeat (NB-LRR) proteins, has been conserved for several hundred million years and features a structure consisting of N-terminal signaling domains, a conserved central nucleotide-binding site, and C-terminal leucine-rich repeats. Plant NB-LRR proteins are structurally and functionally analogous to animal nucleotide-binding leucine-rich repeat receptor (NLR) innate immune receptors (3, 4). NB-LRR receptors recognize pathogen-encoded effector proteins either directly or indirectly via effector action on a host target. This initiates signal transduction and transcriptional reprogramming, resulting in effector triggered immunity and localized hypersensitive-response (HR) cell death (1, 2).

The functions of NB-LRR domains have been intensively investigated, but the mechanisms of NB-LRR activation and subsequent signaling are not well defined (5). A reasonable model has emerged wherein the N-terminal coiled-coil (CC) or Toll-interleukin-1 receptor (TIR) domain, in conjunction with the LRR domain, inhibits nucleotide exchange and/or hydrolysis in the resting state. Effector recognition, whether direct or indirect, results in an "unfurling" of the molecule, altered intra- and intermolecular interactions, changes in association with cochaperones, enhanced nucleotide turnover, and consequent downstream signaling, which occurs by mechanisms that are largely unknown (6–9).

Preactivation NB-LRR proteins have been localized to multiple subcellular compartments (10). NB-LRR activation has been associated with dynamic relocalization. In some cases, a small fraction of the total NB-LRR pool appears to relocalize to the nucleus, where it is thought to regulate defense gene transcription (10). These examples include both coiled coil (CC) (11–13) and TIR-NB-LRR (14–16) proteins and the RRS1 fusion protein that juxtaposes an NB-LRR protein with a WRKY class DNA binding domain (17). To date, however, there is no generalization regarding site(s) of NB-LRR activation or action.

RPM1 is a CC-NB-LRR protein (18). Inactive, signal-competent RPM1 is a plasma membrane-associated protein (19). RPM1 interacts with another plasma membrane localized protein, RIN4. RPM1 recognizes effector-mediated modifications of RIN4 in the presence of the bacterial type III effector proteins AvrRpm1 or AvrB (20, 21). AvrRpm1 and AvrB are also localized to the host plasma membrane by postdelivery acylation, and this localization is required for their ability to modify RIN4 and, consequently, activate RPM1 (22). RIN4 is required for wild-type levels of RPM1 accumulation at the membrane (20) and is a suppressor of weak RPM1 autoactivity (23). Hence, it is plausible that RPM1 activation occurs on the plasma membrane. Whether activated RPM1 relocalizes to initiate downstream signaling is not clear.

In this study, we determine the localization of an autoactive RPM1 allele that mimics accurately the activation state of wild-type RPM1. Collectively, our results indicate that activated RPM1 remains on the plasma membrane and that nuclear localization of RPM1 is not required for its function. Our results focus attention on how the activation state of RPM1 is transduced into an efficient disease resistance response.

Results

Transient Expression of an MHD Domain RPM1 Mutant Allele Induces Cell Death in *Nicotiana benthamiana*. We wanted to address whether RPM1 relocalizes following activation. In principle, pre- and postactivation RPM1 states could coexist in the same cell during activation, due to temporal and spatial differences in signaling mediated by delivery of the relevant effector proteins. We therefore generated an autoactive allele of RPM1 to simplify the analysis of activation and potential consequent relocalization by biochemical methods. Mutations in the conserved MHD motif and Walker B motif can cause autoactivity that is likely achieved by intramolecular conformational rearrangement. We constructed myc-epitope tagged RPM1(D505V) and RPM1(D287A) alleles

Author contributions: Z.G., E.-H.C., and J.L.D. designed research; Z.G., E.-H.C., and T.K.E. performed research; E.-H.C. and T.K.E. contributed new reagents/analytic tools; Z.G., E.-H.C., T.K.E., and J.L.D. analyzed data; and Z.G. and J.L.D. wrote the paper.

The authors declare no conflict of interest.

[1]To whom correspondence should be addressed. E-mail: dangl@email.unc.edu.

This article contains supporting information online at www.pnas.org/lookup/suppl/doi:10.1073/pnas.1104410108/-/DCSupplemental.

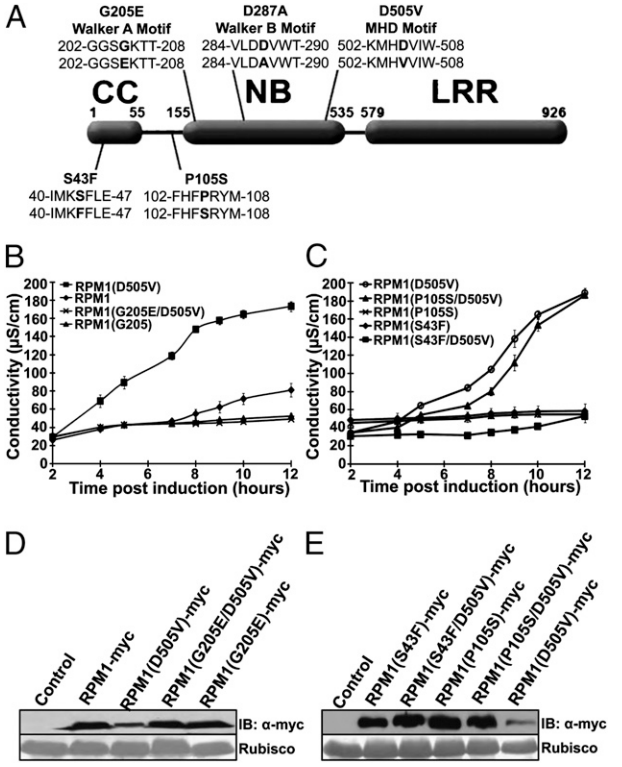

Fig. 1. The MHD domain mutant RPM1(D505V) induces cell death in *N. benthamiana*. (*A*) RPM1 mutants used in this work. Wild-type sequences (*Upper*) and mutant sequences (*Lower*) are shown. (*B* and *C*) Estradiol-inducible RPM1 alleles were transiently expressed in *N. benthamina* (OD_{600} = 0.3). The HR-inducing activity of the RPM1 alleles was measured by ion leakage. (*D* and *E*) RPM1 proteins were detected by immunoblot. Samples were collected at 5 h after the induction with 40 μM estradiol and 40 μg of total extract loaded. Rubisco was used for protein loading control. Protein samples from uninfiltrated leaves were used as a control for nonspecific cross-reactivity.

(Fig. 1*A*). Each was sufficient to induce cell death, as measured by changes in media conductivity, when transiently expressed in *N. benthamiana* (Fig. 1 *B* and *C* and Fig. S1). Because RPM1(D505V) exhibited stronger autoactivity than RPM1(D287A) (Fig. S1*A*), it was used for most of the subsequent experiments.

We also reconstructed three previously isolated RPM1 loss-of-function mutants to test their effects in *cis* on the autoactivity of RPM1 (D505V) (24). The first, RPM1(S43F), is located in the N-terminal coiled-coil domain; the second, RPM1(P105S), is located in a highly variable spacer region; and the third, RPM1 (G205E), is in the Walker A motif (P-loop) domain required for ATP binding. As expected, none of these three mutants is autoactive (Fig. 1*C*). Autoactivity of RPM1(D505V) requires the P-loop motif because it is suppressed in *cis* in RPM1(G205E/D505V) (Fig. 1*B*). This result shows that autoactivation of RPM1(D5050V) mimics P-loop–dependent activation of wild-type RPM1 triggered by type III effectors. Similarly, autoactivity of RPM1(D505V) requires the CC domain because it is also suppressed in RPM1 (S43F/D505V) (Fig. 1*C*). By contrast, RPM1(P105S/D505V) retains autoactivity (Fig. 1*C*), suggesting that the functional requirement for RPM1(P105) occurs before the state in normal RPM1 activation mimicked by RPM1(D5050V). The steady-state abundance of RPM1 (D505V) protein is lower than that of RPM1 or the other mutant alleles (Fig. 1 *D* and *E*). Intramolecular suppression of autoactivation restored wild-type accumulation to RPM1(S43F/D505V). Thus, the low levels of RPM1(D505V) protein are consistent with our previous report that the disappearance of RPM1 is correlated with effector-mediated activation and the onset of HR cell death (19). We noted that two common proteasome inhibitors, MG132 and *clasto*-lactacystin β-lactone, could not stabilize steady-state levels of RPM1(D5050V), suggesting that the disappearance of activated RPM1 is not mediated by the proteasome.

Autoactivity of RPM1(D505V) Can Be Suppressed by RIN4. RIN4 is formally a negative regulator of RPM1 because RPM1 is weakly autoactive in a *rin4* null mutant (23). We co-expressed RIN4 and RPM1(D505V) in *N. benthamiana* to test the effect of RIN4 on the autoactivity of RPM1(D505V). RIN4 was constitutively expressed from its native promoter, and RPM1(D505V) expression was induced with estradiol 2 d after *Agrobacterium* infiltration. Our results showed that RIN4 expression delayed and diminished cell death (Fig. 2*A*). Co-expression of RIN4 also delayed the disappearance of RPM1(D505V) (Fig. 2*B*).

We confirmed and extended these findings by expressing Myc epitope-tagged RPM1(D505V) from its native promoter [*gRPM1 (D505V)-Myc*] in transgenic *Arabidopsis rpm1* or *rpm1 rps2 rin4* plants to test the effects of RIN4 on the autoactivity of RPM1 (D505V) in *Arabidopsis*. Use of *rpm1 rps2 rin4* as a recipient for these experiments, instead of *rpm1 rin4*, is necessary to avoid the lethal ectopic autoactivation of RPS2 in the latter genotype (25). Independent transgenic *gRPM1(D505V)-Myc rpm1* lines exhibited an essentially wild-type growth phenotype (Fig. 2 *C* and *D*) and expressed variable levels of RPM1(D505V). By contrast, independent transgenic *gRPM1(D505V) rpm1 rps2 rin4* lines were difficult to recover, severely stunted as homozygous T2 individuals, expressed RPM1 at very low levels, and typically expressed the PR-1 protein, a marker of ectopic basal defense (Fig. 2 *C* and *D*). The severity of the dwarf phenotype was correlated with RPM1(D505V) levels in *gRPM1(D505V) rpm1 rps2 rin4* T2 transgenic plants (Fig. 2 *C* and *D*). These results support our conclusion that RIN4 can also suppress the autoactivity of RPM1 (D505V) in transgenic *Arabidopsis* (Fig. 2*D*).

RPM1(D505V) levels in *rpm1* transgenic lines were lower than wild-type RPM1 from a well-characterized transgenic line, *gRPM1-Myc rpm1* (19), and were similar to the expression of the same transgene introgressed into *rar1* (Fig. 2*D*). The RAR1 cochaperone is required to maintain wild-type NB-LRR levels. Its absence results in reduced NB-LRR levels that can drop below a threshold required for function (24, 26). Hence, the level of RPM1-Myc detected in *rar1* defines an RPM1 level lower than its functional threshold.

We extended this finding by crossing the dwarfed, PR-1 expressing, single-insertion *gRPM1(D505V)-Myc rpm1 rps2 rin4* line 49 transgene (Fig. 2*C*) into *rpm1 rps2*. The resulting line had a wild-type phenotype, and the expression level of RPM1(D505V) was higher than that of the same transgene in an *rpm1 rps2 rin4* sibling (Fig. 2*E*). The autoactivity of RPM1(D505V) in *rpm1 rps2 rin4* also conferred enhanced basal resistance to the virulent pathogen *Pto* DC3000, and this was suppressed by the presence of RIN4 (Fig. 2*F*). We conclude that RIN4 can partially stabilize RPM1(D505V) and fully suppress its autoactivity of RPM1(D505V).

Effector-Mediated Activation of RIN4-Repressed RPM1(D505V). RPM1 (D505V), repressed by RIN4 in the lines shown in Fig. 2 *C–E*, was reactivated following recognition of AvrRpm1 delivered via the type III secretion system in both HR and growth restriction assays (Fig. S2 *A–C*). RPM1(D505V) levels in these lines are well below that of wild-type RPM1 (Fig. 2*D*). We infer that RPM1(D505V) has higher functional efficiency than wild type following effector-mediated activation. The weaker RPM1(D287A) autoactive allele also supported effector-mediated activation, at least for the ability to trigger HR in *N. benthamiana* (Fig. S1*C*). Thus, the autoactive RPM1 (D505V) allele behaves like wild-type RPM1 with respect to both inhibition by RIN4 and subsequent effector-mediated activation.

Activated RPM1(D505V) Localizes on the *Arabidopsis* Plasma Membrane. We localized RPM1(D505V) in both the presence and the absence of RIN4 in *rpm1* or *rpm1 rps2 rin4* transgenic plants. We separated extracts into soluble and microsomal membrane fractions by ultracentrifugation (20) (Fig. 3*A*). These microsomal fractions were further separated into plasma membranes and

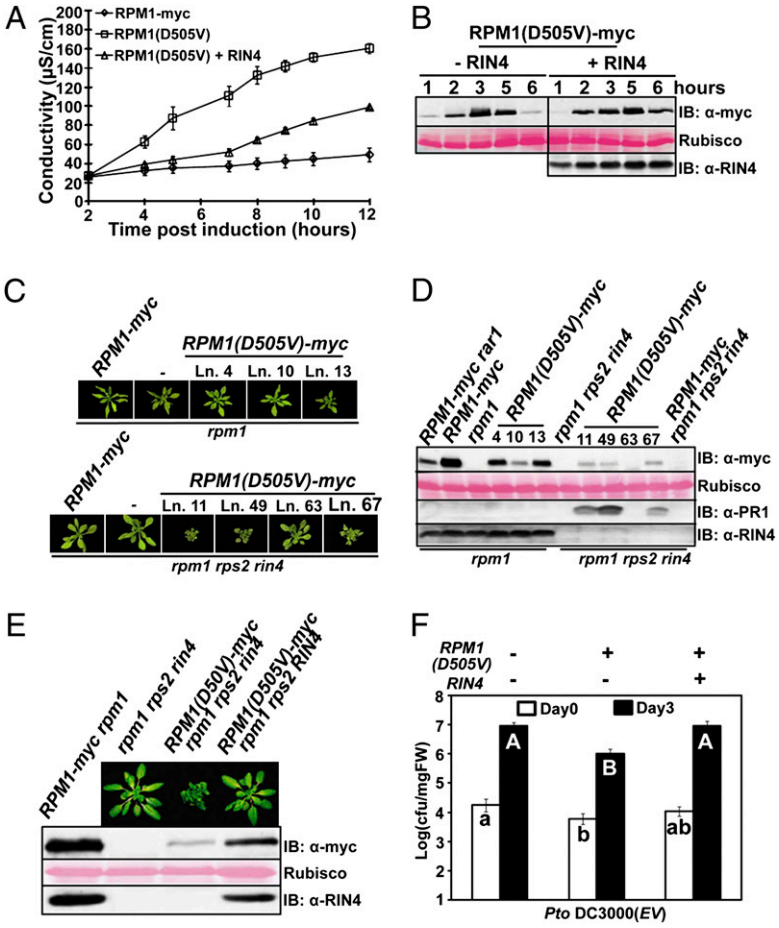

Fig. 2. The autoactivity of RPM1(D505V) is sufficient to trigger enhanced disease resistance and can be suppressed by RIN4. (*A*) Ion leakage induced by transient expression of RPM1 (D505V) with or without RIN4 in *N. benthamiana*. RIN4 is expressed from its native promoter [OD_{600} = 0.3 for RIN4 and OD_{600} = 0.3 for RPM1(D505V) or RPM1]. RPM1(D505V) was induced with 40 μM estradiol. (*B*) RPM1(D505V)-myc expression over a time course after estradiol induction, with or without RIN4 co-expression. (*C*) Pictures of rosettes from *RPM1 (D505V)-myc* transgenic plants (genetic backgrounds noted at top). The plants were grown under 16-h-long days for 6 wk. (*D*) Protein expression levels in the transgenic plants. Samples were collected from 4-wk-old plants grown under 9-h short days. (*E*) Photos and protein expression levels of isogenic *RPM1(D505V)-myc* line 49 plants with or without *RIN4*. Line 49 of *RPM1(D505V)-myc rpm1 rps2 rin4* (*C* and *D*) was crossed with *rpm1 rps2* to obtain isogenic *RPM1(D505V)-myc rpm1 rps2* plants. (*F*) Enhanced disease resistance following inoculation with *Pto* DC3000 of the isogenic plants from *E*. Seedlings were dip-inoculated with 2.5×10^7 cfu/mL of *Pto* DC3000. Pair-wise comparison for all means from day 0 or day 3 values were performed with a one-way ANOVA test coupled with Tukey–Kramer HSD with 95% confidence limits.

endomembranes by two-phase partitioning (27). Like wild-type RPM1 (19), RPM1(D505V) is predominantly localized to the plasma membrane (Fig. 3*B*). It is noteworthy that the autoactive RPM1(D505V) in *rpm1 rps2 rin4* also fractionates to the plasma membrane. This result demonstrates that active RPM1 is retained at the plasma membrane.

Given recent interest in the relocalization of NB-LRR proteins to the nucleus, we also tested whether RPM1(D505V) relocalized to that compartment. We identified no RPM1(D505V) specifically in our nuclear extracts, even when these were overloaded by 20-fold (Fig. 3*C*). Overloading by 20-fold means that if 5% of the total RPM1(D505V) were in the nucleus, then that signal would equal the signal detected in the nuclear depleted lanes of Fig. 3*C*. Thus, our detection limit is significantly less than 5%. These results indicate that it is highly unlikely that activated RPM1 (D505V) relocalizes to the nucleus.

We also established that there is no specific fragment processed from N-terminally tagged autoactive T7-RPM1(D505V)-YFP-HA alleles during its activation (Fig. S3). The results validate our results using C-terminal epitope-tagged RPM1(D505V). The results shown in Fig. 3 and Fig. S3 are consistent with the full-length of RPM1(D505V) being the functional molecule.

RPM1(D505V) Localizes on the Plasma Membrane of *N. benthamiana* Epidermal Cells. We localized the autoactive T7-RPM1(D505V)-YFP-HA and control T7-RPM1-YFP-HA via confocal microscopy. PLC2-CFP was used as a plasma membrane marker (28). The estradiol-induced expression of T7-RPM1(D505V)-YFP-HA caused cell death beginning ~5 h post induction (Fig. S3*A*). Consistent with this, dead or dying epidermal cells of *N. benthamiana* had shrunken shapes under the confocal microscope at this time point (Fig. 4). We observed the localization of RPM1 (D505V) in precisely the same cell over time (Fig. 4). RPM1 (D505V) was localized predominantly on the plasma membrane at 4 and 4.5 h post induction. Epidermal cell shape was unchanged at these time points. RPM1(D505V) levels were reduced, and the epidermal cell exhibited altered morphology at 5 h post induction. There was some alteration in the pattern of the remaining RPM1 (D505V) signal distributed along the plasma membrane, and some redistribution into putative endomembrane structures at the 5-h time point. Because the plasma membrane marker PLC2 colocalized with RPM1(D505V) in the endomembrane structures, and because the translocation of PLC2 occurred only when the cell began to die, these endomembrane structures are likely to be a consequence of cell death, rather than a signaling intermediate. Preactivation T7-RPM1-YFP-HA was stably localized on the plasma membrane throughout this time course.

Excluding the Entry of RPM1 into the Nucleus Does Not Block Its Function. We further confirmed that RPM1(D505V) neither relocalizes to, nor functions in, the nucleus, using nuclear export signal (NES)-tagged *RPM1-Myc-NES* under the control of the native RPM1 promoter (*gRPM1-Myc-NES*) (*Materials and Methods*) (11). We generated stable transgenic *gRPM1-Myc-NES rpm1* and *gRPM1-Myc-nes rpm1* plants and tested for effector-mediated HR and disease resistance functions over a range of expression levels. The efficiency of RPM1 function in either assay was determined by the RPM1 expression level, and not by the NES or mutant (nes) tag, indicating that the NES sequence does not alter RPM1 function (Fig. S4). Addition of a nuclear localization signal (NLS) onto these NES-tagged molecules affected localization, but did not alter function (Fig. S5). The nuclear localization of NLS-RPM1-GFP-NES was reduced, compared with that of NLS-RPM1-GFP-nes, showing that the NES tag is functional. How-

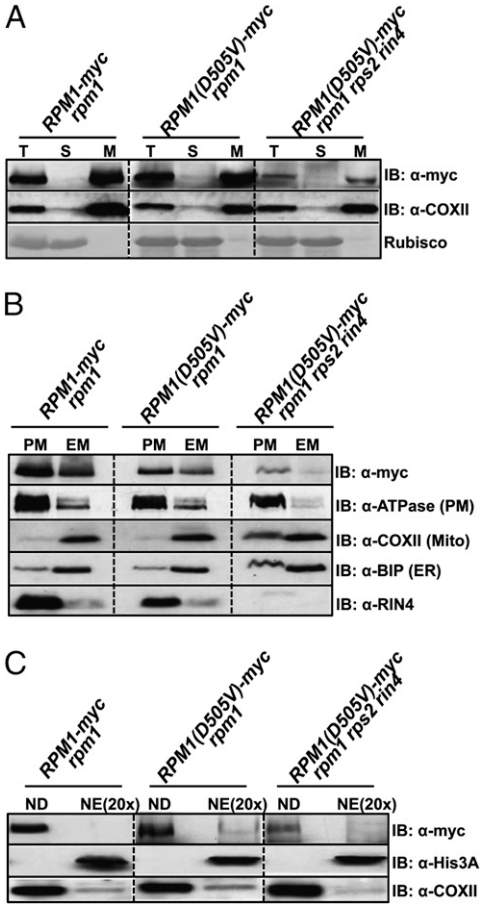

Fig. 3. RPM1(D505V) localizes on the plasma membrane in *Arabidopsis*. (*A*) RPM1(D505V) resides on microsomal membranes. Total protein (T) was separated into soluble (S) and microsomal membrane (M) fractions by ultracentrifugation. COXII, a mitochondria membrane protein, was used as a membrane protein marker. Rubisco was used as a soluble protein marker. (*B*) RPM1(D505V) resides on the plasma membrane. The microsomal membrane fraction (M) was further separated into the plasma membrane fraction (PM) and the endomembrane fraction (EM). H^+-ATPase, COXII, and Bip were used as plasma membrane, mitochondrial membrane, and endoplasmic reticulum markers, respectively. (*C*) RPM1(D505V) is not in the nuclear fraction. RPM1(D505V) was present in nuclear depleted (ND) but not in nuclear enriched (NE) fractions. Histone 3A was used as a nuclear protein marker. COXII was used as a non-nuclear marker. Note that NE fractions are loaded at a 20× yield equivalent compared with ND fractions. Three grams of leaves from plants grown under 16-h-long days for 6 wk were used for the experiments. The leaves of *RPM1(D505V) rpm1* and *RPM1(D505V) rpm1 rps2 rin4* are from line 4 and line 11, respectively (Fig. 2*D*).

ever, the two proteins exhibited the same efficiency for effector-mediated HR. These data also support the contention that, under these expression conditions, the HR function of RPM1 does not require relocalization to the nucleus.

Plasma Membrane-Tethered RPM1 Retains HR Function in *N. benthamiana*. If translocation of RPM1 from the plasma membrane to other subcellular locations is necessary for its function, then a plasma membrane-tethered RPM1 should exhibit reduced function. The first 12 amino acids of CBL1 (calcineurin B-like protein 1) can target proteins to the plasma membrane due to myristoylation on G2 and palmitoylation on C3 (29). We added this 12-amino-acid peptide (i.e., CBL) to the N terminus of several RPM1-Myc derivatives to tether them to the plasma membrane. A mutant CBL (mCBL) that could not be acylated was made as a control (Fig. 5*A*). We surprisingly found that ~50% of the RPM1(G205E/D505V) P-loop mutant described

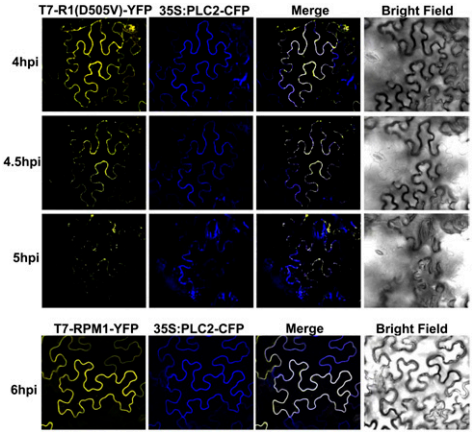

Fig. 4. T7-RPM1(D505V)-YFP localizes to the plasma membrane of *N. benthamiana* epidermal cells. Transient expression of T7-RPM1(D505V)-YFP or T7-RPM1-YFP (OD_{600} = 0.3) was induced with 20 μM estradiol at 48 h after agrobacteria infiltration. Images were collected at the time after induction noted at left. 35S:PLC2-CFP (OD_{600} = 0.3) was co-expressed as a plasma membrane marker.

above (Fig. 1) was soluble (Fig. 5*B*), whereas, as noted in Fig. 4, both RPM1 and RPM1(D505V) were strictly membrane localized. We used this result to test whether the CBL tag could retether the soluble RPM1(G205E/D505V) protein to the membrane. CBL, but not mCBL, efficiently tethered the soluble RPM1(G205E/D505V) to the membrane (Fig. 5*B*). Two-phase partitioning demonstrated that CBL-RPM1(G205E/D505V) was localized to the plasma membrane (Fig. 5*D*). Both CBL-RPM1 and mCBL-RPM1 were also retained on plasma membrane localization (Fig. 5 *C* and *D*).

Constitutive overexpression of CBL-RPM1, but not of mCBL-RPM1 or RPM1, led to weak autoactivity in *N. benthamiana* compared with effector-activated HR of the same molecules (compare Fig. 5*E* to Fig. S6). Accumulation of CBL-RPM1 was lower than that of either mCBL-RPM1 or RPM1, consistent with weak autoactivation (Fig. S6). Hence, the weak autoactivity observed with CBL-tagged RPM1, but not with mCBL-tagged RPM1, is likely due to the dual lipid modification rather than to the mere pres ence of the N-terminal tag. The weak autoactivity of CBL-RPM1 was suppressed by co-expression with RIN4 (Fig. S6), making this molecule a useful tool to test whether tethering RPM1 to the plasma membrane alters effector-mediated activation of HR.

We thus co-expressed in *N. benthamiana* CBL-RPM1 under the control of the 35S promoter and RIN4 under the control of its native promoter and then conditionally induced AvrRpm1 36 h post infiltration. CBL-RPM1-Myc supported nearly wild-type levels of effector-mediated HR (Fig. 5*E*). mCBL-RPM1 was less efficient than CBL-RPM1. The functional difference between CBL-RPM1 and mCBL-RPM1 could suggest that the dual-lipid modification of the CBL tag has positive effects on both autoactivity and effector-mediated RPM1-dependent HR, which partially compensates for any negative effects of the N-terminal tag. CBL-RPM1(G205E/D505V) did not support effector-mediated RPM1-dependent HR, indicating that HR requires a functional nucleotide-binding site, but that retethering the largely soluble RPM1(G205E/D505V) to the plasma membrane is insufficient to rescue the P-loop loss-of-function mutation. We conclude that the robust HR function of CBL-RPM1 indicates that plasma membrane-tethered RPM1 retains its HR function.

Discussion

This study was motivated by the question of how NB-LRR proteins, specifically RPM1, are activated by pathogen effectors, or by the activity of pathogen effectors on associated host targets, and whether activation is accompanied by dynamic relocalization of some or all of the active RPM1. Detailed analyses of this kind

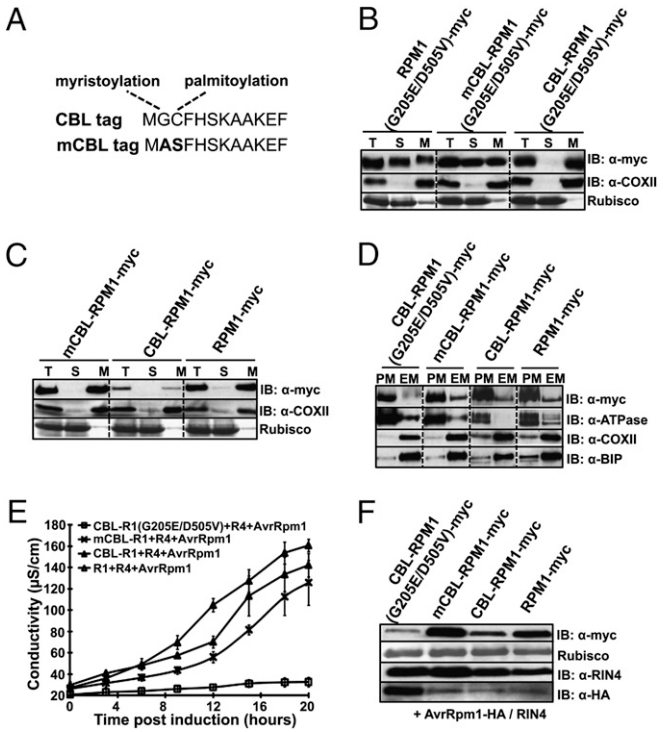

Fig. 5. Plasma membrane-tethered RPM1 retains effector-mediated HR function in *N. benthamiana*. (*A*). CBL tag contains dual-lipid modification sites. (*B*) The CBL tag tethers soluble RPM1(G205E/D505V)-Myc to the microsomal membrane following conditional transient expression in *N. benthamiama*. (*C*) CBL and mCBL tags do not affect the membrane localization of RPM1-Myc. (*D*) CBL-tagged proteins localize on the plasma membrane. For *B–D*, proteins were transiently expressed in *N. benthamiana* under the control of 35S promoter (OD_{600} = 0.5). Samples were collected at 40 h after agrobacteria infiltration. (*E*) The HR function of CBL-tagged RPM1. CBL- or mCBL-tagged RPM1-myc (R1) under the control of 35S promoter, T7-RIN4 (R4) under the control of its native promoter and AvrRpm1-HA (AvrRpm1) under the control of a dexamethasone (Dex)-inducible promoter were co-expressed in *N. benthamiana* (OD_{600} = 0.5, 0.3, and 0.05, respectively). AvrRpm1 was induced with 20 μM Dex at 36 h after infiltration. (*F*) The expression level of the constructs. The protein levels of the tagged RPM1 and RIN4 were detected at 2 h after induction. The protein levels of AvrRpm1 were detected at 6 h after induction.

are still rare for plant NB-LRR proteins, and generalities have proven difficult to establish (5, 10).

Here, we used both transient and stable transgenic expression in transgenic *Arabidopsis* at native levels to establish that an autoactive RPM1(D505V) allele resides on the plasma membrane and does not obviously relocalize. The autoactivity of this allele is P-loop–dependent, suggesting that its activation proceeds by a mechanism similar to the activation of RPM1 by type III effectors. The autoactivity of RPM1(D505V) was repressed by RIN4 in both experimental systems. RIN4-repressed RPM1(D505V) could still be activated by the type III effector AvrRpm1. Hence, RPM1 (D505V) autoactivity is a reasonable proxy for activation of wild-type RPM1. Our cell fractionation and confocal microscopy results indicate that activated RPM1 resides solely on the plasma membrane and is not detectable in the nucleus under conditions where we can easily detect less than 5% of RPM1 protein in the cell. Autoactive alleles in the MHD domain of NB-LRR proteins are likely to be generically useful tools to identify the endogenous partners and regulators of NB-LRR proteins and to sequence activation steps with subcellular localization.

We also tethered RPM1 onto the plasma membrane using a N-terminal dual-acylation sequence. This RPM1 derivative retained the ability to trigger HR in response to AvrRpm1 in the presence of RIN4. Collectively, our results suggest that activated RPM1 resides on the plasma membrane, that effector-mediated activation of RPM1 occurs on the plasma membrane, and, finally, that anchoring RPM1 to the plasma membrane does not significantly alter its HR induction function. Our results are consistent with the conclusion that RPM1 function does not require nuclear translocation for function.

At least two other NB-LRR receptors are likely to act at the plasma membrane. Pit is a CC-NB-LRR protein that is active against rice blast fungus. An analogous MHD domain allele, Pit (D485V), is autoactive in *N. benthamiana*. Confocal images from rice protoplasts indicated that Pit and Pit(D485D) are plasma membrane-localized (30). Pit interacts with Rac1; Pit(D485V), but not Pit, activated Rac1 (a regulator of reactive oxygen species production and cell death) on the plasma membrane, suggesting that activated Pit also initiates signal transduction on the plasma membrane (30). The plasma membrane-localized CC-NB-LRR protein RPS2 also associates with RIN4 at the membrane, and the relevant type III effector, AvrRpt2, is also likely to be acylated and localized to the plasma membrane, suggesting that the activation of RPS2 also starts on the plasma membrane. Effector-activated RPS2 is stable and localized to a microsomal compartment, although it is not clear whether this is actually the plasma membrane (25, 31).

We report the surprising finding that the P-loop is important for RPM1 localization. We noted that ~50% of RPM1(G205E/D505V) was soluble and lacked autoactivity, compared with the nearly complete plasma membrane association of both RPM1 and RPM1(D505V). Notably, CBL-RPM1(G205E/D505V) is still a complete loss-of-function allele even though it is tethered to the plasma membrane. Thus, mutations in the RPM1 P-loop affect both localization and function. Consistent with this, the P-loop is required for intramolecular interactions of Rx (32), oligomerization of N (33), and direct interaction of L6 with the AvrL6 effector protein (34). The wide effects of P-loop mutations on NB-LRR function are therefore likely to reflect not only the necessity of nucleotide binding to maintain a functional resting state conformation, but also the correct localization of that optimal conformer for each NB-LRR protein.

RIN4 interacts with the CC domain of RPM1 (20). RIN4 could suppress the autoactivity of RPM1(D505V) either by blocking a required conformational change involving the CC domain or by blocking the interaction of RPM1 with downstream signaling components. The CC domain of RPM1 is critical for function (24). Similarly, the CC domain of the barley powdery mildew A NB-LRR immune receptor MLA interacts with WRKY transcription factors, and a CC dimer is both necessary and sufficient for signaling and required for the interaction of MLA with the WRKY transcription factors (35). These examples provide evidence that the CC domain of NB-LRR immune receptors can provide functions that may change during activation and can demonstrably act in different subcellular contexts. Similar findings are suggested for TIR domains (36) and for the noncanonical N terminus of Prf (37), focusing future work on understanding how these domains act as sensors of both effector-mediated target modification and initiators of downstream signaling.

Animal NLR proteins are also found in diverse subcellular locations, require analogous chaperones to maintain preactivation competence, and can relocalize upon activation to participate in a variety of signaling complexes. The mammalian CIITA NLR protein functions in the nucleus (38–40). NOD2 is present at, and recruits a downstream partner to, the plasma membrane; a mutation in its LRR renders NOD2 cytosolic and nonfunctional (41). NOD1 and NOD2 recruit autophagy components focally to plasma membrane sites of bacterial infection, and a common NOD2 variant associated with Crohn's disease fails to do so (42). These studies reveal that mammalian NLRs localize to different places in the cell before activation, that they can dynamically relocalize, and that their cellular localization influences downstream function. The sum of the data from plant NB-LRR and animal NLR intracellular immune receptors is consistent with the conceptual role of NB-LRR proteins as monitors of cellular ho-

meostasis surveying a wide array of cellular defense machineries across a variety of subcellular addresses (1).

Materials and Methods

Plant Growth Conditions. *Arabidopsis* plants used for HR and disease resistance experiments were grown at 24 °C under a 8-h light/16-h dark cycle. Plants for other purposes and *N. benthamiana* plants were grown in a greenhouse at 24 °C under a 16-h light/8-h dark cycle.

Vectors. Vectors used in this study were constructed as described in *SI Materials and Methods*.

Transient Protein Expression in *N. benthamiana*. *Agrobacterium*-mediated transient expression assays in *N. benthamiana* are described in *SI Materials and Methods*.

Total Protein Extraction and Primary Antibodies. Total protein was extracted with extraction buffer [20 mM Tris·HCl (pH 7.5), 150 mM NaCl, 1 mM EDTA, 1% SDS, 10 mM DTT]. The supernatant after centrifugation at 9,000 × *g* for 3 min was used for Western blot. The primary antibodies used were anti-Myc (University of North Carolina, Chapel Hill), anti-GFP (Roche), anti-HA (Roche), anti-T7 (Novagen), anti-COXII (Agrisera), anti–H^+-ATPase (Agrisera), anti-Bip (Santa Cruz Biotechnology), anti-RIN4 (20), and anti-histone H3 (Abcam; ab1791). Anti-PR-1 (a gift from X. Dong, Duke University, Durham, NC).

Membrane Fractionation and Isolation of Nuclei. Two-phase partitioning was performed as previously described (27) with a few modifications as described in *SI Materials and Methods*. Plant nuclei were isolated with a plant nuclei isolation kit (Sigma-Aldrich). Semipure preparation of nuclei was performed according to the protocol (Sigma-Aldrich).

HR and Disease Resistance Assays. For conductivity assays, four leaf discs (0.8-cm diameter) were collected and floated in 5 mL of water with three replicates per sample (n = 12) at 2 h after induction with estradiol or dexmethasone. Ion leakage was measured at indicated time points using a conductivity meter (Orion; model 130). For HR assay, the leaves of 5-wk-old plants were infiltrated with *Pto* DC3000(*avrRpm1*) at 5×10^7 cfu/mL. The leaves were stained with Trypan blue 6 h after infiltration (43). Bacterial growth was measured as described (44).

Confocal Microscopy. The localization of T7-RPM1(D505V)-YFP and T7-RPM1-YFP was observed under confocal microscopy (LSM 510 Meta; Carl Zeiss) as described in *SI Materials and Methods*.

ACKNOWLEDGMENTS. We thank Professors Roger Innes and John McDowell for critical reading, and members of the Dangl/Grant laboratory for helpful discussions. This work was funded by National Science Foundation Arabidopsis 2010 Program Grants IOS-0929410 and DOE DE-FG05-95ER20187 (to J.L.D.). T.K.E. was supported by a National Institutes of Health Training Grant.

1. Jones JD, Dangl JL (2006) The plant immune system. *Nature* 444:323–329.
2. Dodds PN, Rathjen JP (2010) Plant immunity: Towards an integrated view of plant-pathogen interactions. *Nat Rev Genet* 11:539–548.
3. Ting JP, Willingham SB, Bergstralh DT (2008) NLRs at the intersection of cell death and immunity. *Nat Rev Immunol* 8:372–379.
4. Vance RE, Isberg RR, Portnoy DA (2009) Patterns of pathogenesis: Discrimination of pathogenic and nonpathogenic microbes by the innate immune system. *Cell Host Microbe* 6:10–21.
5. Eitas TK, Dangl JL (2010) NB-LRR proteins: Pairs, pieces, perception, partners, and pathways. *Curr Opin Plant Biol* 13:472–477.
6. Takken FLW, Albrecht M, Tameling WIL (2006) Resistance proteins: Molecular switches of plant defence. *Curr Opin Plant Biol* 9:383–390.
7. van Ooijen G, et al. (2008) Structure-function analysis of the NB-ARC domain of plant disease resistance proteins. *J Exp Bot* 59:1383–1397.
8. Takken FL, Tameling WI (2009) To nibble at plant resistance proteins. *Science* 324: 744–746.
9. Shirasu K (2009) The HSP90-SGT1 chaperone complex for NLR immune sensors. *Annu Rev Plant Biol* 60:139–164.
10. Caplan J, Padmanabhan M, Dinesh-Kumar SP (2008) Plant NB-LRR immune receptors: From recognition to transcriptional reprogramming. *Cell Host Microbe* 3:126–135.
11. Shen QH, et al. (2007) Nuclear activity of MLA immune receptors links isolate-specific and basal disease-resistance responses. *Science* 315:1098–1103.
12. Tameling WI, et al. (2010) RanGAP2 mediates nucleocytoplasmic partitioning of the NB-LRR immune receptor Rx in the Solanaceae, thereby dictating Rx function. *Plant Cell* 22:4176–4194.
13. Slootweg E, et al. (2010) Nucleocytoplasmic distribution is required for activation of resistance by the potato NB-LRR receptor Rx1 and is balanced by its functional domains. *Plant Cell* 22:4195–4215.
14. Burch-Smith TM, et al. (2007) A novel role for the TIR domain in association with pathogen-derived elicitors. *PLoS Biol* 5:e68.
15. Wirthmueller L, Zhang Y, Jones JD, Parker JE (2007) Nuclear accumulation of the Arabidopsis immune receptor RPS4 is necessary for triggering EDS1-dependent defense. *Curr Biol* 17:2023–2029.
16. Cheng YT, et al. (2009) Nuclear pore complex component MOS7/Nup88 is required for innate immunity and nuclear accumulation of defense regulators in Arabidopsis. *Plant Cell* 21:2503–2516.
17. Tasset C, et al. (2010) Autoacetylation of the Ralstonia solanacearum effector PopP2 targets a lysine residue essential for RRS1-R-mediated immunity in Arabidopsis. *PLoS Pathog* 6:e1001202.
18. Grant MR, et al. (1995) Structure of the *Arabidopsis RPM1* gene enabling dual specificity disease resistance. *Science* 269:843–846.
19. Boyes DC, Nam J, Dangl JL (1998) The *Arabidopsis thaliana RPM1* disease resistance gene product is a peripheral plasma membrane protein that is degraded coincident with the hypersensitive response. *Proc Natl Acad Sci USA* 95:15849–15854.
20. Mackey D, Holt BF, III, Wiig A, Dangl JL (2002) RIN4 interacts with Pseudomonas syringae type III effector molecules and is required for RPM1-mediated resistance in Arabidopsis. *Cell* 108:743–754.
21. Chung EH, et al. (2011) Specific threonine phosphorylation of a host target by two unrelated type III effectors activates a host innate immune receptor in plants. *Cell Host Microbe* 9:125–136.
22. Nimchuk Z, et al. (2000) Eukaryotic fatty acylation drives plasma membrane targeting and enhances function of several type III effector proteins from *Pseudomonas syringae*. *Cell* 101:353–363.
23. Belkhadir Y, Nimchuk Z, Hubert DA, Mackey D, Dangl JL (2004) Arabidopsis RIN4 negatively regulates disease resistance mediated by RPS2 and RPM1 downstream or independent of the NDR1 signal modulator and is not required for the virulence functions of bacterial type III effectors AvrRpt2 or AvrRpm1. *Plant Cell* 16:2822–2835.
24. Tornero P, Chao RA, Luthin WN, Goff SA, Dangl JL (2002) Large-scale structure-function analysis of the Arabidopsis *RPM1* disease resistance protein. *Plant Cell* 14:435–450.
25. Mackey D, Belkhadir Y, Alonso JM, Ecker JR, Dangl JL (2003) Arabidopsis RIN4 is a target of the type III virulence effector AvrRpt2 and modulates RPS2-mediated resistance. *Cell* 112:379–389.
26. Bieri S, et al. (2004) RAR1 positively controls steady state levels of barley MLA resistance proteins and enables sufficient MLA6 accumulation for effective resistance. *Plant Cell* 16:3480–3495.
27. Larsson C, Sommarin M, Widell S (1994) Isolation of highly purified plant plasma membranes and separation of inside-out and right-side-out vesicles. *Methods Enzymol* 228:451–469.
28. Hirayama T, Mitsukawa N, Shibata D, Shinozaki K (1997) AtPLC2, a gene encoding phosphoinositide-specific phospholipase C, is constitutively expressed in vegetative and floral tissues in Arabidopsis thaliana. *Plant Mol Biol* 34:175–180.
29. Batistic O, Sorek N, Schültke S, Yalovsky S, Kudla J (2008) Dual fatty acyl modification determines the localization and plasma membrane targeting of CBL/CIPK Ca2+ signaling complexes in Arabidopsis. *Plant Cell* 20:1346–1362.
30. Kawano Y, et al. (2010) Activation of a Rac GTPase by the NLR family disease resistance protein Pit plays a critical role in rice innate immunity. *Cell Host Microbe* 7:362–375.
31. Axtell MJ, Staskawicz BJ (2003) Initiation of *RPS2*-specified disease resistance in Arabidopsis is coupled to the AvrRpt2-directed elimination of RIN4. *Cell* 112:369–377.
32. Moffett P, Farnham G, Peart J, Baulcombe DC (2002) Interaction between domains of a plant NBS-LRR protein in disease resistance-related cell death. *EMBO J* 21:4511–4519.
33. Mestre P, Baulcombe DC (2006) Elicitor-mediated oligomerization of the tobacco N disease resistance protein. *Plant Cell* 18:491–501.
34. Dodds PN, et al. (2006) Direct protein interaction underlies gene-for-gene specificity and coevolution of the flax resistance genes and flax rust avirulence genes. *Proc Natl Acad Sci USA* 103:8888–8893.
35. Maekawa T, et al. (2011) Coiled-coil domain-dependent homodimerization of intracellular barley immune receptors defines a minimal functional module for triggering cell death. *Cell Host Microbe* 9:187–199.
36. Bernoux M, et al. (2011) Structural and functional analysis of a plant resistance protein TIR domain reveals interfaces for self-association, signaling and autoregulation. *Cell Host Microbe* 9:200–211.
37. Gutierrez JR, et al. (2010) Prf immune complexes of tomato are oligomeric and contain multiple Pto-like kinases that diversify effector recognition. *Plant J* 61:507–518.
38. Cressman DE, Chin KC, Taxman DJ, Ting JP (1999) A defect in the nuclear translocation of CIITA causes a form of type II bare lymphocyte syndrome. *Immunity* 10:163–171.
39. Zhu XS, et al. (2000) Transcriptional scaffold: CIITA interacts with NF-Y, RFX, and CREB to cause stereospecific regulation of the class II major histocompatibility complex promoter. *Mol Cell Biol* 20:6051–6061.
40. Harton JA, Cressman DE, Chin KC, Der CJ, Ting JP (1999) GTP binding by class II transactivator: Role in nuclear import. *Science* 285:1402–1405.
41. Lécine P, et al. (2007) The NOD2-RICK complex signals from the plasma membrane. *J Biol Chem* 282:15197–15207.
42. Travassos LH, et al. (2010) Nod1 and Nod2 direct autophagy by recruiting ATG16L1 to the plasma membrane at the site of bacterial entry. *Nat Immunol* 11:55–62.
43. Koch E, Slusarenko A (1990) Arabidopsis is susceptible to infection by a downy mildew fungus. *Plant Cell* 2:437–445.
44. Tornero P, Dangl JL (2001) A high-throughput method for quantifying growth of phytopathogenic bacteria in *Arabidopsis thaliana*. *Plant J* 28:475–481.

Supporting Information

Gao et al. 10.1073/pnas.1104410108

Supporting Information Corrected May 19, 2011

SI Materials and Methods

Vector Constructs. The Myc sequence is directly fused to the 3′ sequence of RPM1 by PCR from the pGPTV-HPT binary vector (1). The GFP sequence was fused to the 3′ sequence of RPM1 by NotI ligation. The nuclear export signal (NES) sequence or nes sequence (2) was fused to the 3′ sequence of myc or GFP by PCR. The nuclear localization signal (NLS) sequence, CBL sequence, mutant CBL (mCBL), or T7 sequence was fused to the 5′ sequence of RPM1 by PCR. The promoter region of RPM1 (1 kb) was fused to the 5′ sequence of RPM1 by PCR. The constructs of *gRPM1 (D505V)-myc*, *gRPM1-myc-NES*, and *gRPM1-myc-nes* were in a Gateway vector pGWB1 (3). Estradiol-inducible expression constructs were in the Gateway vector pMDC7 (4) or pMDC7-YFP-HA (YFP-HA sequence was fused to pMDC7 by PacI and SpeI ligation). Constructs using the 35S promoter were in the Gateway vector pGWB2 (3). The Dex:AvrRpm1-HA construct was described previously (5). The T7 epitope sequence was fused to the 5′ cDNA sequence of RIN4. The promoter region of RIN4 (1.6 kb) was fused to the 5′ sequence of T7-RIN4. The construct was in a pBAR1-GW destination vector (6). The pBAR1-GW was constructed by inserting a Gateway cassette (Invitrogen) into the multicloning sites of pBAR1 with HindIII and SacI ligation. The construct of 35S:PLC2-CFP was a gift from E. Washington (University of North Carolina, Chapel Hill). The following sequences were used:

NES: 5′-atggacgagctgtacaagaacgagcttgctcttaagttggctggacttgat-attaacaag-3′;
nes: 5′-atggacgagctgtacaagaacgagcttgctcttaaggcagctggagcagat-gctaacaag-3′;
NLS: 5′-ggaccaaagaagaaacggaaggtc-3′;
CBL: 5′-atgggctgcttccactcaaaggcagcaaaagaattt-3′;
mCBL: 5′-atggccagcttccactcaaaggcagcaaaagaattt-3′;
T7: 5′-atggctagcatgactggtggacagcaaatgggt-3′.

***Agrobacterium*-Mediated Transient Assay.** *Agrobacterium tumefaciens* strain GV3101 containing protein expression binary plasmid constructs was grown overnight at 28 °C with suitable antibiotics. Cells were resuspended in induction media [10 mM Mes (pH 5.6), 10 mM $MgCl_2$, and 150 μM actosyringone] and incubated at room temperature for 2 h before infiltration. Co-infiltrated *Agarobacteria* were mixed together to the desired final OD_{600} values and were infiltrated into the leaves of 5- to 6-wk-old *Nicotiana benthamiana* with a 1-mL needleless syringe. *Agarobacterium* containing the p19-expression plasmid (7) was always co-infiltrated with other agrobacteria at a final OD_{600} of 0.2.

Aqueous Two-Phase Partitioning. Tissue was homogenized in a mortar on ice with lysis buffer [0.33 M sucrose, 50 mM Tris·HCl (pH 7.5), 5 mM EDTA, 5 mM DTT, and protease inhibitor mixture (Sigma-Aldrich)]. The lysate was filtered with one-layer miracloth and was further cleared with centrifugations at 2,000 × *g* for 5 min and 6,000 × *g* for 10 min. The supernatant was fractioned into a soluble fraction and microsomal membrane fraction with ultracentrifugation at 100,000 × *g* for 30 min.: The fresh microsomal fraction was suspended in a suspension buffer [0.33 M sucrose, 5 mM potassium phosphate buffer (pH 7.8), 3 mM KCl, and protease inhibitor mixture (Sigma-Aldrich)]. The suspended membrane was mixed with the two-phase solution (8) at a ratio of 1:5 (w/w). The final polymer concentration was 6.1% (w/w).

Confocal Microscopy. Agrobacteria expressing T7-RPM1(D505V)-YFP and T7-RPM1-YFP were infiltrated in *N. benthaminana* leaves. Leaf discs (5-mm diameter) were floated in water with 20 μM estradiol for 3 h. The abaxial sides of leaves were observed with a confocal microscope (LSM 510 Meta; Carl Zeiss). Images were collected every 30 min. YFP fluorescence was excited at 514 nm and detected between 530 and 600 nm. CFP fluorescence was excited at 458 nm and detected between 480 and 520 nm. For observing the nuclear localization of RPM1-GFP, the infiltrated leaves were induced with 20 μM of estradiol for 8 h. DAPI (10 μg/mL) was infiltrated into the leaves 30 min before confocal observation. GFP fluorescence was excited at 488 nm and observed between 505 and 530 nm. DAPI fluorescence was excited at 375 nm and observed between 385 and 470 nm. All samples were imaged with a 40× oil objective.

1. Boyes DC, Nam J, Dangl JL (1998) The *Arabidopsis thaliana RPM1* disease resistance gene product is a peripheral plasma membrane protein that is degraded coincident with the hypersensitive response. *Proc Natl Acad Sci USA* 95:15849–15854.
2. Shen QH, et al. (2007) Nuclear activity of MLA immune receptors links isolate-specific and basal disease-resistance responses. *Science* 315:1098–1103.
3. Nakagawa T, et al. (2007) Development of series of gateway binary vectors, pGWBs, for realizing efficient construction of fusion genes for plant transformation. *J Biosci Bioeng* 104:34–41.
4. Curtis MD, Grossniklaus U (2003) A gateway cloning vector set for high-throughput functional analysis of genes in planta. *Plant Physiol* 133:462–469.
5. Mackey D, Holt BF III, Wiig A, Dangl JL (2002) RIN4 interacts with Pseudomonas syringae type III effector molecules and is required for RPM1-mediated resistance in Arabidopsis. *Cell* 108:743–754.
6. Chung EH, et al. (2011) Specific threonine phosphorylation of a host target by two unrelated type III effectors activates a host innate immune receptor in plants. *Cell Host Microbe* 9:125–136.
7. Voinnet O, Rivas S, Mestre P, Baulcombe D (2003) An enhanced transient expression system in plants based on suppression of gene silencing by the p19 protein of tomato bushy stunt virus. *Plant J* 33:949–956.
8. Larsson C, Sommarin M, Widell S (1994) Isolation of highly purified plant plasma membranes and separation of inside-out and right-side-out vesicles. *Methods Enzymol* 228:451–469.

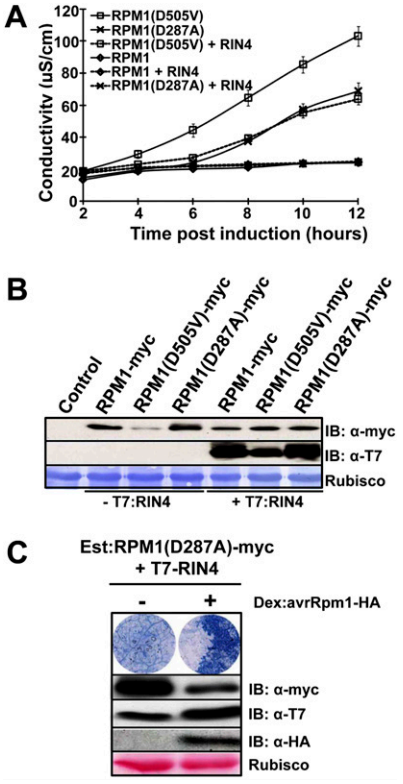

Fig. S1. Autoactivity and hypersensitive-response (HR) functions of RPM1(D287A). (*A*) RIN4 co-expression represses the autoactivity of both RPM1(D55V) and RPM1(D287A). Estradiol-inducible RPM1 alleles were transiently expressed in *N. benthamina* (OD_{600} = 0.3). T7-RIN4 under the control of its native promoter was co-expressed (OD_{600} = 0.3) with RPM1 mutants to determine the effects of RIN4 on the autoactivity of RPM1 (D287A). (*B*) The expression levels of the RPM1 mutants and T7-RIN4. (*C*) Effector-mediated activation of RPM1(D287A)-myc. Estradiol-inducible RPM1(D287A)-myc and T7-RIN4 and Dex-inducible AvrRpm1-HA (OD_{600} = 0.3, 0.3, and 0.05 respectively) were co-expressed in *N. benthamiana*. The leaf discs were stained with Trypan blue at 7 h after induction with 20 μM of estradiol and 20 μM of Dex. Protein expression levels in 40 μg of total extract were detected at 5 h after induction.

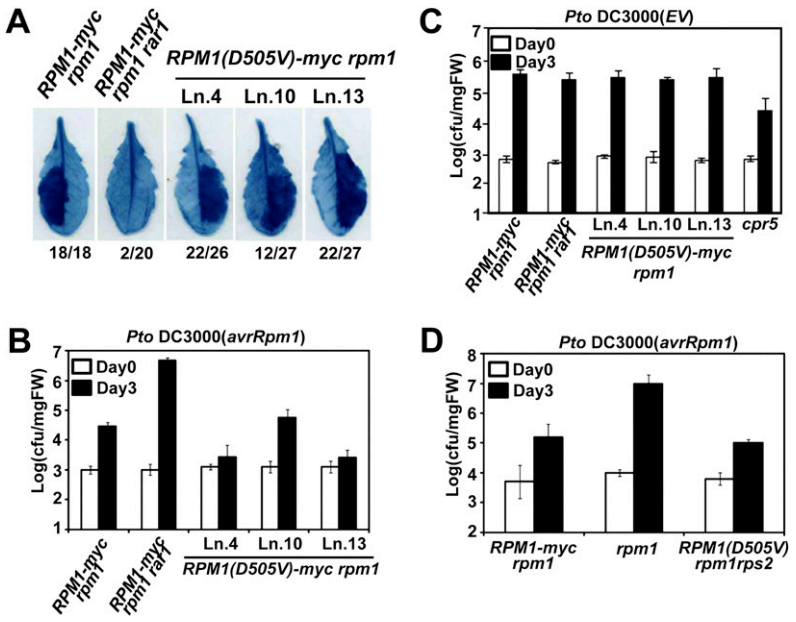

Fig. S2. Effector-activated hypersensitive response (HR) and disease resistance are retained by RPM1(D505V). (*A*) The HR function of RPM1(D505V). Leaves from transgenic lines 4, 10, and 13 (Fig. 2 *C* and *D*) were infiltrated with 5×10^7 cfu/mL *Pto* DC3000 (*avrRpm1*) and stained with Trypan blue at 6 h after infiltration. The number of leaves exhibiting HR over the total number inoculated is shown. (*B*) The disease resistance function of RPM1(D505V). Seedlings from the transgenic lines noted were dip-inoculated with 2.5×10^7 cfu/mL of *Pto* DC3000(*avrRpm1*). (*C*) The effects of RPM1(D505V) on plant basal defense. Same transgenic lines as in *B* were dip-inoculated with 2.5×10^7 cfu/mL of *Pto*DC3000(*EV*). No significant difference was observed. The constitutive pathogen response 5 (*cpr5*) mutant was used as control for enhanced disease resistance. (*D*) Line 49 transgene *RPM1(D505V)-myc rpm1 rps2* plants (Fig. 2*E*) retain effector-triggered disease resistance. Inoculations as in *B*.

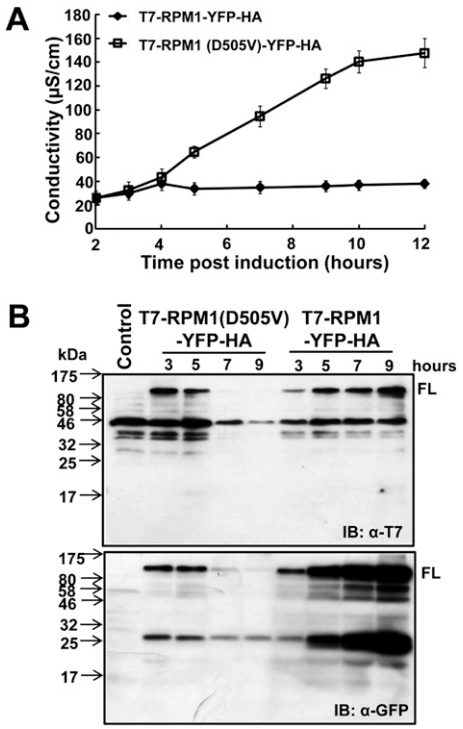

Fig. S3. The full-length RPM1(D505V) protein autoactivates hypersensitive response. Results that rely on detection of C-terminal epitope-tagged RPM1 will be valid under the important assumption that RPM1 or RPM1(D505V) functions as a full-length protein. However, if a C-terminally truncated RPM1(D505V) is the activated molecule, then we would not be able to detect this with anti-Myc antibody. To determine whether RPM1(D505V) functions as a full-length protein, we constructed a conditionally expressed, double epitope-tagged version of RPM1(D505V) called T7-RPM1(D505V)-YFP-HA. We used the N-terminal T7 tag to detect potential C-terminal truncations and the C-terminal YFP-HA tag to detect potential N-terminal truncations. Importantly, the T7-RPM1(D505V)-YFP-HA protein retains autoactivity, whereas a control T7-RPM1-YFP-HA is not active following transient expression in *N. benthamiana*. We did not observe specific truncated fragments of T7-RPM1(D505V)-YFP-HA during a time course following estradiol induction leading to the onset of cell death, although by 7 h post induction the activated protein has largely disappeared (*B*). (*A*) The autoactivity of T7-RPM1(D505V)-YFP-HA. The protein was transiently expressed in *N. benthamiana* (OD_{600} = 0.3). Cell death was detected with ion leakage. (*B*) Protein expression of T7-RPM1(D505V)-YFP-HA over time. The full-length T7-RPM1 (D505V)-YFP-HA (marked as FL) and possible C-terminal truncations were detected with anti-T7 antibody. The full-length T7-RPM1(D505V)-YFP-HA and the possible N-terminal truncations were detected with anti-GFP antibody. T7-RPM1-YFP-HA was used as a negative control. Protein samples from uninfiltrated leaves were used as the control of immunoblot.

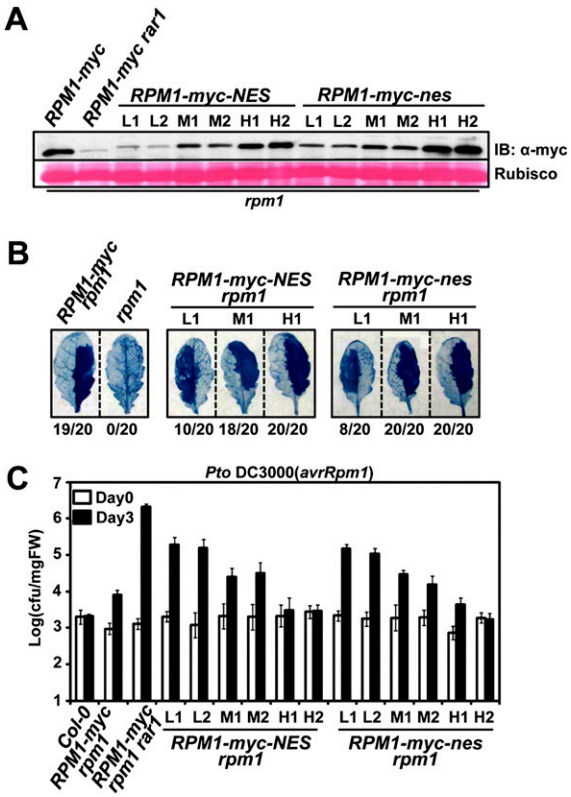

Fig. S4. RPM1-Myc-NES has hypersensitive-response (HR) and disease-resistance functions. (*A*) Expression levels of RPM1-Myc-NES and RPM1-Myc-nes in independent, nonsegregating T3 transgenic *rpm1* plants. Transgenic plants were grouped into high (H), medium (M), and low (L) expression categories. (*B*) The HR function of RPM1-Myc-NES is retained. The leaves were infiltrated with 5×10^7 cfu/mL of *Pto* DC3000(*avrRpm1*) and stained with Trypan blue at 6 h after infiltration. The number of leaves exhibiting HR over the total number inoculated is shown. (*C*) The disease-resistance function of RPM1-Myc-NES is retained. Seedlings were dip-inoculated with 2.5×10^7 cfu/mL of *Pto* DC3000(*avrRpm1*).

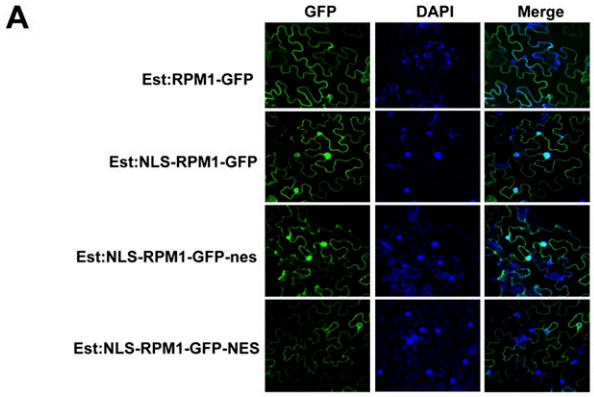

B

	nucleus	ring	no/weak	total
RPM1-GFP	0	0	31	31
NLS-RPM1-GFP	29	1	10	40
NLS-RPM1-GFP-NES	5	18	19	42
NLS-RPM1-GFP-nes	23	5	6	34

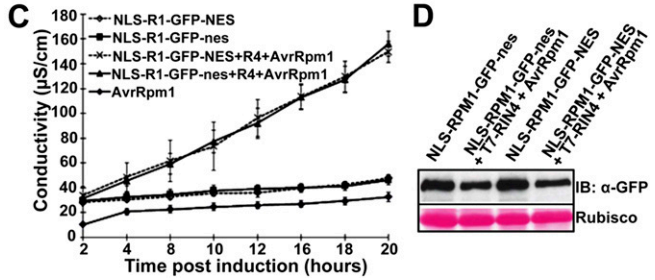

Fig. S5. The NES tag is functional and can export nuclear localized NLS-RPM1-GFP out of the nucleus. Because there is no detectable RPM1 signal in the nucleus (Fig. 3*C* and Fig. 4), we added an NLS (*Materials and Methods*) to the N terminus of RPM1-GFP (Est:*NLS-RPM1-GFP*). This NLS efficiently localized NLS-RPM1-GFP into the nucleus following transient expression in *N. benthamiana* (*A* and *B*). We further constructed Est:*NLS-RPM1-GFP-NES* and Est:*NLS-RPM1-GFP-nes* and tested whether the NES could efficiently export NLS-RPM1-GFP-NES out of the nucleus. The nuclear localization of NLS-RPM1-GFP-NES was obviously lower than that of NLS-RPM1-GFP-nes, suggesting that the NES is sufficient to export NLS-RPM1-GFP out of the nucleus. The peri-nuclear accumulation of NLS-RPM1-GFP-NES is consistent with previous observations (*A* and *B*) (1). Importantly, although neither NLS-RPM1-GFP-NES nor NLS-RPM1-GFP-nes were autoactive, they did respond to AvrRpm1 and initiate hypersensitive response (HR) in the presence of RIN4 (*C* and *D*). (*A*) The effects of NLS and NES tags on RPM-1-GFP localization. Constructs of RPM1 noted at left were co-expressed with T7-RIN4 into *N. benthamiana* leaves (OD_{600} = 0.5 for RPM1 constructs and OD_{600} = 0.3 for T7-RIN4). Estradiol (20 μM) was painted onto the leaves at 48 h after agrobacteria infiltration. Confocal imaging began at 8 h after estradiol induction. The nuclei of the epidermal cells were stained with DAPI at 10 μg/mL. The NLS tag drives some RPM1 into the nucleus, the NES tag can export this protein, and this export requires a functional NES. (*B*) Quantification of microscopy results from *A*. The number of cells that showed GFP signal in the nucleus, a perinuclear ring, or neither (no/weak) is given. Data are from three independent experiments. (*C*) NLS-RPM1-GFP-NES and NLS-RPM1-GFP-nes retain effector-triggered HR. Estradiol-inducible NLS-RPM1-GFP-NES or NLS-RPM1-GFP-nes, T7-RIN4, and Dex-inducible AvrRpm1-HA (OD_{600} = 0.5, 0.3, and 0.05, respectively) were co-expressed in *N. benthamiana*. Transient expression of proteins was induced with 20 μM estradiol and 20 μM Dex at 48 h after agrobacteria infiltration. (*D*) Expression level of NLS-RPMGFP-NES and NLS-RPM1-GFP-nes was detected at 5 h after estradiol induction.

1. Shen QH, et al. (2007) Nuclear activity of MLA immune receptors links isolate-specific and basal disease-resistance responses. *Science* 315:1098–1103.

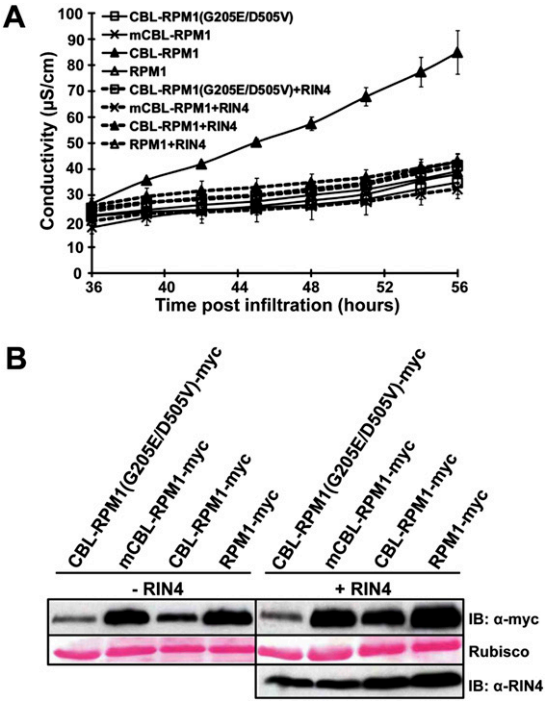

Fig. S6. CBL-RPM1-Myc has weak autoactivity. (*A*) The weak autoactivity of CBL-RPM1-Myc. RPM1 constructs controlled under the 35S promoter were transiently expressed in *N. benthamiana* with or without co-expression of native promoter T7-RIN4 (OD_{600} = 0.5 for RPM1 constructs and OD_{600} = 0.3 for T7-RIN4). Cell death was monitored with ion leakage. (*B*) Protein expression level of RPM1 constructs and RIN4. Samples were collected at 36 h after infiltration.